Atomic and local electronic structure of Gd thin films studied by STM and STS

R. Pascal, Ch. Zarnitz, M. Bode, and R. Wiesendanger
Institute of Applied Physics and Microstructure Research Center, University of Hamburg, Jungiusstrasse 11, D-20355 Hamburg, Germany
(Received 6 May 1997)

We report on combined scanning tunneling microscopy and spectroscopy studies of the atomic and local electronic structure of Gd thin films on W(110) in the submonolayer coverage regime. The tunneling spectra of a recent (8×2), and the previously known (7×2), (6×2), (5×2) and $c(5\times3)$ superstructures show significant differences in the local electronic structure, which were found to be due to the varying interatomic distances within the Gd film. Spatially resolved maps of the tunneling barrier height reveal a nonmonotonic behavior of the local work function from the open (8×2) structure to the close-packed first monolayer. [S0163-1829(97)05731-7]

Thin-film and surface studies of Gd as a prototypical ferromagnetic $4f$ rare-earth metal have recently attracted considerable interest because of its interesting surface magnetic properties. For instance, an enhancement of the Curie temperature of the surface compared to the bulk ($T_{CB}=293$ K) was observed based on spin-polarized low-energy electron diffraction,[1] magneto-optical Kerr effect (MOKE),[2] and spin-polarized secondary-electron emission spectroscopy studies.[3] The electronic structure of Gd films was investigated by angle-resolved photoemission and inverse photoemission experiments,[4] as well as by spin-resolved photoelectron spectroscopy.[5] A strong change in the $5d$ state and, along with it, of the core levels with decreasing film thickness down to approximately 1.5 ML was revealed,[6] as was the existence of a surface state at about 0.3 eV above the Fermi level E_F. Furthermore, a nonvanishing exchange-splitting even at room temperature of the unoccupied $5d$ state could be confirmed[7] in agreement with the observation of an enhanced surface magnetic order. The annealing conditions of Gd films, deposited at room temperature, were found to have a strong influence on the magnetic properties, as shown by MOKE (Refs. 8 and 9) and ac magnetic susceptibility measurements on films of 5–11 ML thickness.[8] This indicates the importance of the relationship between topographical and magnetic structure of the films. It was suggested, that for Gd deposited on W(110) at 300 K the growth mode is a nonideal layer-by-layer growth, while annealing at temperatures around 500 K leads to a well-ordered film. Raising the annealing temperature to around 720 K leads to formation of three-dimensional (3D) islands on top of 1 ML Gd. A recent scanning tunneling microscopy (STM) study of Gd on W(110) in the coverage regime of 1–20 ML addressed the issue of the correlation between surface morphology and magnetic properties and could explain the magnetic susceptibility data based on the two possible growth modes of Gd on W(110) for different annealing conditions.[10,11] Although Gd(0001) films on W(110) have been intensively studied in the past for the coverage regime of one up to several ML, very little is known about the submonolayer coverage regime.

In this report, we present a combined STM and scanning tunneling spectroscopy (STS) study of the atomic and local electronic structure of Gd on W(110) in the submonolayer coverage regime. The STM data reveal (10×2), (7×2), (6×2), (5×2), and $c(5\times3)$ superstructures, being in excellent agreement with earlier structure models based on low-energy electron diffraction (LEED) data.[10] In addition, an (8×2) superstructure has been discovered by STM and LEED, for which a structure model is proposed. Simultaneously recorded tunneling spectra reveal significant differences in the local electronic structure for these five superstructures. A systematic change in the spectra is observed by decreasing the distance between Gd chains of the (8×2) to the (5×2) superstructure. In addition, spatially resolved measurements of the tunneling barrier height have been performed which reveal a nonmonotonic behavior of the local work function by going from the open (8×2) to the close-packed monolayer of Gd. It is found that the (5×2) and (6×2) superstructures exhibit the lowest local work function on the nanometer scale in agreement with earlier measurements performed on a macroscopic scale.[10]

The STM /STS experiments were performed in a multichamber ultra-high vacuum system with a base pressure in the low 10^{-11} Torr range. The W(110) crystal was cleaned by heating in oxygen and flashing up to 2600 K. Gd thin films were prepared by evaporation from a tungsten crucible heated by electron-beam bombardment.[12] The Gd films were found to be free of carbon and oxygen within the detection limit of Auger electron spectroscopy and LEED. During evaporation, the pressure did not rise above 2×10^{-10} Torr. Post annealing of the films, evaporated at room temperature, was performed in the temperature range between 520 and 720 K. Topographic STM images were obtained in the constant current mode of operation. Tunneling spectra were measured in constant height mode with lock-in technique by applying a small modulation voltage of $U_{\mathrm{mod}}=20$ mV at a frequency $\nu=1.4$ kHz to the sample bias voltage. Spatially resolved maps of the tunneling barrier height were obtained by modulating the vertical position of the STM tip with $\Delta z=0.3$ Å at $\nu_{\mathrm{mod}}=1.8$ kHz and using lock-in technique as for the spectroscopic measurements.

Figure 1 shows a topographic STM image of a 60 × 60 nm^2 area of a nominally 0.5 ML Gd film on W(110) annealed at 710 K for 10 min. Five different surface structures

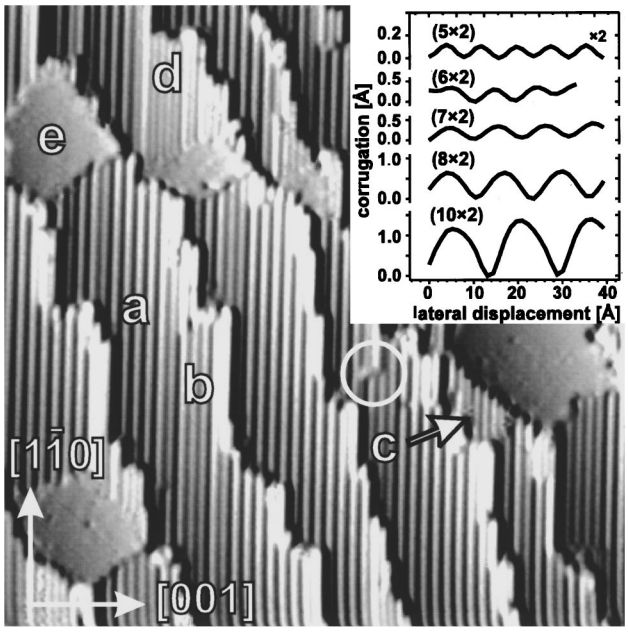

FIG. 1. Constant current STM topograph (scan range: 60×60 nm^2) of 0.5 ML Gd on W(110) annealed at 710 K. Different superstructures are observed at different locations, (*a*) (8×2), (*b*) (7×2), (*c*) (6×2), (*d*) (5×2), and (*e*) $c(5\times3)$. The circle marks a dislocation. Tunneling current $I=1$ nA, sample bias voltage $U=-0.8$ V. The upper right inset displays section lines through the different superstructures along the [001] direction which were obtained with the same tunneling parameters, except for the (10×2) structure ($U=-0.7$ V, $I=1$ nA).

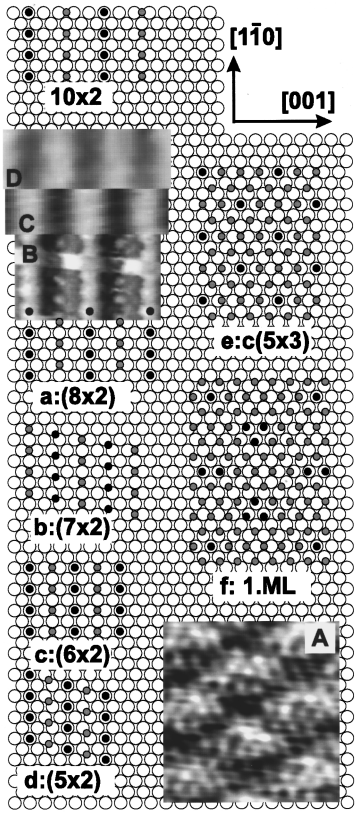

FIG. 2. Atomic structure models of the superstructures formed by Gd/W(110) adopted from Ref. 10, except for the (8×2) superstructure discovered in the present STM study and the close-packed first ML of Gd (Ref. 11). For better clarity of the registry between the two lattices the Gd atoms have been represented as smaller dots. Gd atoms residing in relatively higher positions than their neighbors are shown in black. Inset *A* shows an atomically resolved STM image of the first monolayer. The tunneling parameters are $U=4$ mV, $I=50$ nA. Inset *B* shows the (8×2) superstructure atomically resolved with $U=10$ mV, $I=3$ nA. Insets *C* and *D* display the same structure imaged at -1.2 and 1.2 V, $I=1$ nA, to illustrate the corrugation inversion. The insets are scaled according to the atomic model. The errors with respect to the STM calibration were smaller than 10% for *A* and 3% for *B*, *C*, and *D*.

(labeled *a*–*e*) are visible corresponding to (*a*) (8×2), (*b*) (7×2), (*c*) (6×2), (*d*) (5×2), and (*e*) $c(5\times3)$ superstructures of the thin Gd film. The $(n\times2)$ superstructures are characterized by atomic chains of Gd orientated along the [110] direction of the W(110) substrate. The upper right inset displays section lines through the different superstructures to show the varying interchain distances. The measured periodicities along the [001] direction and the structure-model-based periodicities (in brackets) are (10×2), 15.4±0.5 Å (15.80 Å); (8×2), 12.6±0.1 Å (12.64 Å); (7×2), 10.7±0.5 Å (11.06 Å); (6×2), 9.2±0.3 Å (9.48 Å); and (5×2), 7.8 ±0.3 Å (7.90 Å). The vertical corrugation of the chainlike superstructures, as seen by STM, does not represent the atomic corrugation but is rather an electronic effect, as will be shown later. The formation of chainlike superstructures for submonolayer Gd on W(110) is in strong contrast to the formation of compact 2D islands as usually observed at the early stages of metal on metal growth, as e.g., for Fe on W(110).[13,14] Based on LEED investigations of Kolaczkiewicz and Bauer[10] structure models for the (10×2), (7×2), (6×2), (5×2), and $c(5\times3)$ superstructures were proposed earlier as displayed in Fig. 2 together with a structure model for the first monolayer of Gd on W(110) as proposed by Tober *et al.*[11] Our STM—and LEED—data are fully consistent with the structure models concerning the chainlike superstructures and the pseudohexagonal $c(5\times3)$ superstructure. Additionally, we have added a corresponding structure model for the new (8×2) superstructure as observed in region (*a*) of Fig. 1. An atomic resolution STM image of this superstructure is shown as inset *B* in Fig. 2. It is in excellent agreement with our structure model. The reason why in the submonolayer coverage regime of Gd on W(110) linear chainlike structures are energetically more favorable than compact 2D islands is most likely a repulsive interaction between Gd atoms as proposed earlier in Ref. 10. The adsorption of the electropositive rare-earth metal Gd on W(110), a surface with a relatively high work function, results in a dipole moment of the Gd atoms perpendicular to the substrate surface. Repulsive dipole-dipole interactions can become dominant if it is assumed that the energetic differences between different adsorption sites of Gd on W(110) are small enough so that dipole-dipole repulsive forces can move the Gd atoms away from the adsorption potential minima. The bonding between the Gd atoms in the [110] direction of the W(110) substrate seems to be much stronger than in the [001] direction. This is supported by the fact that dislocations within the rows (marked in Fig. 1 by a circle) only seldomly occur. However, at higher local coverage the Gd atoms have to move closer which results in the quasihex-

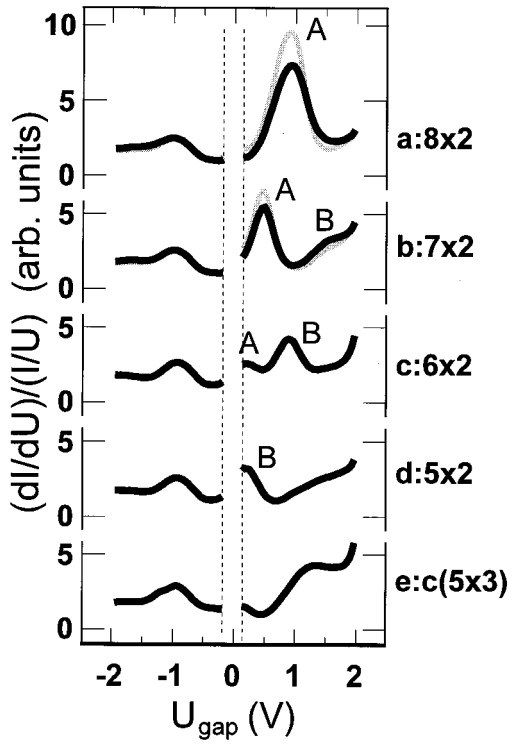

FIG. 3. Normalized tunneling spectra as measured for the five different superstructures observed in the STM image of $a-e$ in Fig. 1 and averaged over the corresponding surface areas except for spectra a and b, where the black curve corresponds to tunneling sites above the maxima of the corrugation and the gray curve to tunneling sites above the minima, as seen at -0.8 V.

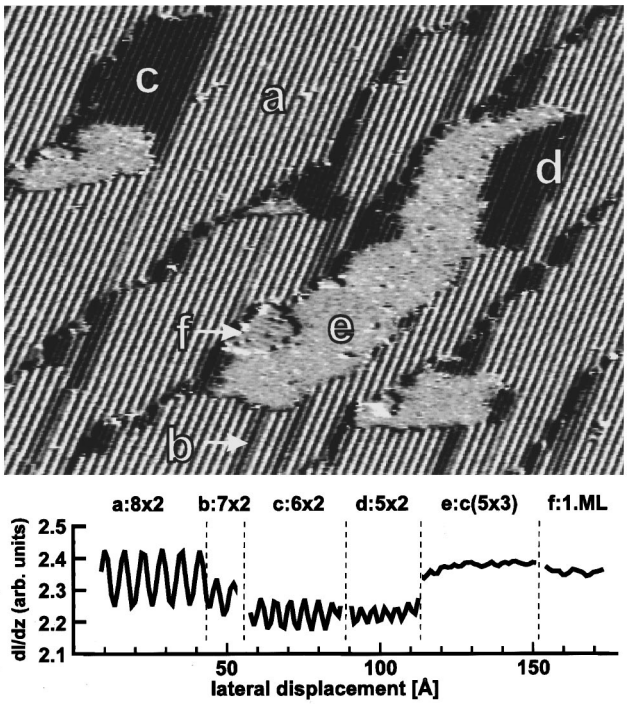

FIG. 4. Spatially resolved map (80×60 nm^2) of the tunneling barrier height reflecting spatial variations in the local surface work function obtained at -0.7 V, 1 nA. The letters mark the same superstructures as in Figs. 1 and 2. The lowest barrier height is measured above the (5×2) and (6×2) superstructures, in agreement with work function measurements (Ref. 10). The inset displays section lines through the dI/dz map for the different superstructures.

agonal $c(5\times3)$ superstructure and finally in the close-packed first ML for which an atomic resolution STM image is displayed as inset A in Fig. 2. Insets C and D display the (8×2) superstructure at a tunneling bias of -1.2 and 1.2 V, respectively. Obviously, the corrugation as measured in the constant current mode becomes inverted. The observation of a significant bias dependence of the topographic STM data which was observed for all one-dimensional superstructures and the $c(5\times3)$ superstructure (data not shown) gave us a clear indication that the STM contrast is mainly determined by the local electronic structure for the different superstructures of Gd on W(110). Therefore, we have performed STS measurements by simultaneously recording topographic data and the normalized differential tunneling conductance $(dI/dU)/(I/U)$ as a function of the applied sample bias voltage U. In Fig. 3 we have plotted the tunneling spectra $(a)-(e)$ corresponding to the superstructures $(a)-(e)$ of Figs. 1 and 2. These spectra have been averaged over the whole surface area on which the corresponding superstructures have been observed. Since the normalization procedure leads to problems around zero bias the region from -0.2 to 0.2 V has been omitted. For the (8×2) and (7×2) superstructures we made a distinction of tunneling sites above the Gd chains representing on-top (bridge) positions, respectively, and chains representing hollow positions. This was possible due to the relatively large interchain distance for these structures. For the more dense structures we found no significant difference between these two sites. By comparing the tunneling spectra $(a)-(e)$ obtained for the submonolayer coverage regime, strong differences are observed, particularly for the empty states for which peak positions as well as peak intensities show a strong dependence on surface structure. A systematic trend in peak positions and intensities seems to be present by going from the (8×2) superstructure with a relatively large interchain distance to the (5×2) structure with the smallest interchain distance. In spectrum (a) we observe a strong peak A at $U\approx1$ eV. The strong peak in spectrum b, labeled A, may be interpreted as the peak A of spectrum a shifted towards E_F due to the decreased interchain distance. This interpretation is supported by the observation that this trend continues for peak A as well as for a new peak B by going to the next closest structure, i.e., (6×2) in spectrum c. Peak B also shifts towards E_F by going from the (6×2) to the (5×2). The spectrum e of the pseudohexagonal $c(5\times3)$ structure does not follow this trend, indicating that it exhibits different local electronic properties. While the electronic structure changes with the interchain distance, different adsorption sites of Gd atoms with respect to the atomic structure of the substrate (gray and black curves in Fig. 2) exhibit only small differences in the electronic structure. For occupied sample states, we observe little changes in tunneling spectra $a-e$. This result may be caused by the fact that tunneling spectroscopy is less sensitive to occupied than to unoccupied sample states.[15]

Additional information about the local electronic structure of the Gd films on W(110) in the submonolayer regime was gained from spatially resolved measurements of the local tunneling barrier height which reflect spatial inhomogeneities in the local surface work function. Figure 4 shows a

barrier height map of 0.5 ML Gd on W(110) that exhibits the same superstructures $a-e$ already known from the STM image of Fig. 1. Additionally, a small surface area f with the structure of a close-packed first ML is observed. At the bottom of Fig. 4 six section lines of the different superstructures in the dI/dz map are displayed. Obviously, the tunneling barrier height and, therefore, the local work function decreases with decreasing interchain distance $a-d$ by going from the (8×2) to the (5×2) superstructure. However, the next dense structure, the $c(5\times3)$, shows a distinctly higher work function compared to the (5×2) structure. This STM-based result on the nanometer scale is in excellent agreement with work-function measurements reported earlier by Kołaczkiewicz and Bauer.[10] They observed the work-function minimum to be associated with the maximum development of the (5×2) and (6×2) LEED pattern of a W(110) sample onto which Gd was continuously evaporated. While spatial averaging of different superstructures is inherent by using this method, the STM offers the possibility to directly observe the change of the local work function for each individual superstructure.

In summary, we have presented an STM study of the different surface structures of Gd on W(110) in the submonolayer coverage regime. This system offers the chance to study the dependence of the electronic structure on interchain distance which constitutes the one-dimensional analogue to the two-dimensional multilayer structures. Tunneling spectroscopy measurements revealed significant and systematic changes in the local electronic structure by going from the quasi-one-dimensional (8×2) structure with relatively large Gd interchain distance to the quasi-one-dimensional (5×2) structure exhibiting the smallest Gd chain separation. To our knowledge, no theoretical electronic structure calculations for chains of atoms resembling Gd or other rare-earth metals are available yet, but are hopefully motivated by the present experimental study.

We would like to thank D. Weller for providing the construction plans for the Gd evaporation source. Financial support by the Deutsche Forschungsgemeinschaft (Grant No. Wi 1277/3-1) and the Graduiertenkolleg ''Nanostrukturierte Festkörper'' is gratefully acknowledged.

[1] D. Weller *et al.*, Phys. Rev. Lett. **54**, 1555 (1985).
[2] M. Farle, W. A. Lewis, and K. Baberschke, Appl. Phys. Lett. **62**, 2728 (1993).
[3] H. Tang *et al.*, Phys. Rev. Lett. **71**, 444 (1993).
[4] E. Weschke *et al.*, Phys. Rev. Lett. **77**, 3415 (1996).
[5] D. Li *et al.*, J. Appl. Phys. **79**, 5838 (1996).
[6] D. Li *et al.*, J. Appl. Phys. **70**, 6565 (1991).
[7] A. V. Fedorov, K. Starke, and G. Kaindl, Phys. Rev. B **50**, 2739 (1994).
[8] M. Farle and W. A. Lewis, J. Appl. Phys. **75**, 5604 (1994).
[9] M. Farle *et al.*, Phys. Rev. B **47**, 11 571 (1993).
[10] J. Kołaczkiewicz and E. Bauer, Surf. Sci. **175**, 487 (1986).
[11] E. D. Tober, R. X. Ynzunza, C. Westphal, and C. S. Fadley, Phys. Rev. B **53**, 5444 (1996).
[12] D. Weller, Ph.D. thesis, Cologne, 1985.
[13] H. Bethge *et al.*, Surf. Sci. **331-333**, 878 (1995).
[14] M. Bode, R. Pascal, M. Dreyer, and R. Wiesendanger, Phys. Rev. B **54**, R8385 (1996).
[15] R. Wiesendanger, *Scanning Probe Microscopy and Spectroscopy* (Cambridge University Press, Cambridge, England, 1994).